$$S_T = \frac{\cos\theta_w}{\sqrt{\cos^2\theta_w + (k_V/k_H)\sin^2\theta_w}}\left(S_w + S_{\text{ani}}\right) + S_\theta \tag{3.26}$$

For usual angles, the skin S_θ is not less than -2 or -3. For very large angles, the response tends towards the horizontal well response, and S_θ can be lower. When the vertical permeability k_V is low compared to k_H, θ_w' is small and the geometrical skin S_θ becomes negligible. In such cases, the effect of the anisotropy is more pronounced and S_{ani} can be more negative than S_θ.

In the following tables, geometrical skin S_θ and S_{ani} are estimated in a reservoir of thickness h =1000 r_w.

Table 3.4. Geometrical skin S_θ

k_V / k_H	1	10^{-1}	10^{-2}	10^{-3}
θ=30°	-0.8	-0.1	0	0
θ=60°	-3.3	-0.9	-0.1	0

Table 3.5. Anisotropy skin S_{ani}

k_V / k_H	1	10^{-1}	10^{-2}	10^{-3}
θ=30°	0	0	-0.1	-0.1
θ=60°	0	-0.3	-0.4	-0.4

3.5.3 Associated specialized plot straight lines

In theory, the two radial flow regimes can be analyzed using semi-log straight line techniques. The first defines the average permeability in the plane normal to the well, multiplied by the well penetration length. In practice, only the second regime, corresponding to horizontal flow from the producing interval, is seen. Semi-log analysis yields the permeability thickness product k_H h of the producing zone and the total skin factor S_T.

3.6 HORIZONTAL WELL

Advances in drilling and completion technologies have placed horizontal wells among the techniques used to improve production performance. For example in the case of gas cap or bottom water drive, horizontal wells prevent coning without introducing the flow restriction seen in partial penetration wells. Horizontal drilling is also efficient to increase the well surface area for fluid withdrawal, thus improving the productivity.

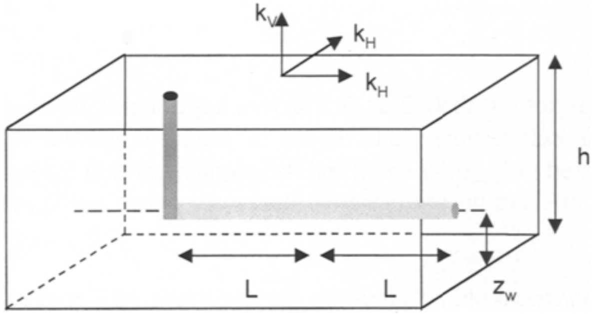

3.6.1 Model description

In this section, we consider first the pressure behavior of horizontal wells in homogeneous reservoirs with sealing upper and lower boundaries. As shown in Figure 3.24 the well is strictly horizontal, the penetration half-length is L and z_w defines the distance between the drain hole and the bottom-sealing boundary. The vertical part of the well is not perforated, there is no flow towards the end of the well and the well conductivity is infinite. k_H and k_V are the horizontal and the vertical permeability.

Characteristic flow regimes

In an infinite system, the geometry of the flow lines towards a horizontal well produces a sequence of three typical regimes, as depicted in Figure 3.25. On the corresponding pressure and derivative response illustrated in Figure 3.26, three characteristic behaviors are displayed after the wellbore storage unit slope straight line:

1. The first regime is *radial flow in the vertical plane*. On a log-log derivative plot, the wellbore storage hump is followed by a first stabilization. During this radial flow regime, the permeability-thickness product $2\sqrt{k_V \cdot k_H}\,L$ is defined with the average permeability in the vertical plane, and the well effective length $2L$.

2. When the sealing upper and lower limits are reached, a *linear flow* behavior is established. The derivative follows a half-unit slope log-log straight line.

3. Later, the flow lines converge from all reservoir directions towards the well, producing a *horizontal radial flow* regime. The derivative stabilization corresponds to the infinite acting radial flow in the reservoir, the permeability-thickness product is k_H h.

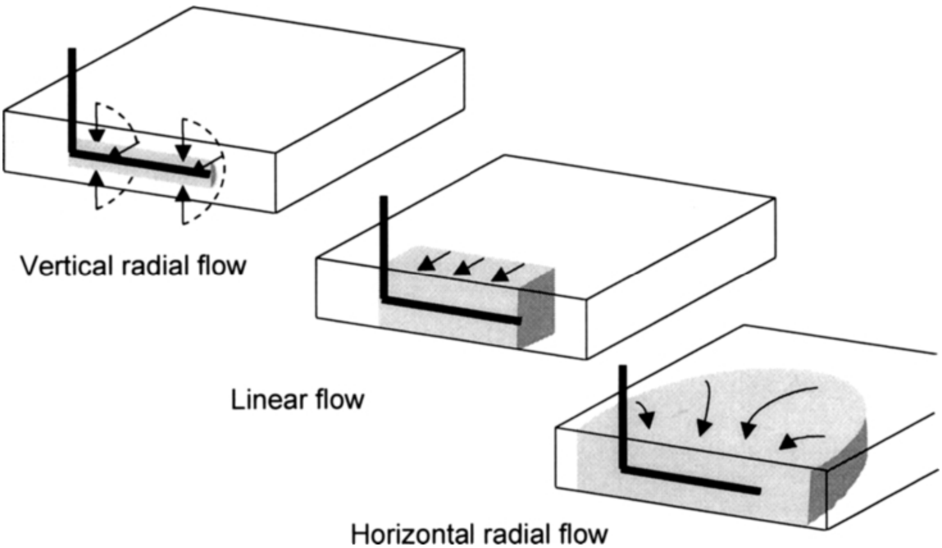

Figure 3.25. Flow geometry to an horizontal well.

Extensions of the model

In practice, the well geometry is not as simple as in the ideal configuration described on Figure 3.24. Most horizontal drain holes are not straight and parallel to the upper and lower boundaries, but show several oscillations over the formation thickness. Frequently, the skin is not uniform along the drain hole and in many cases the well does not produce on the complete length but in one or several segments. When the pressure gradient in the wellbore become large, the infinite conductivity hypothesis is not applicable and the horizontal well shows a finite conductivity behavior.

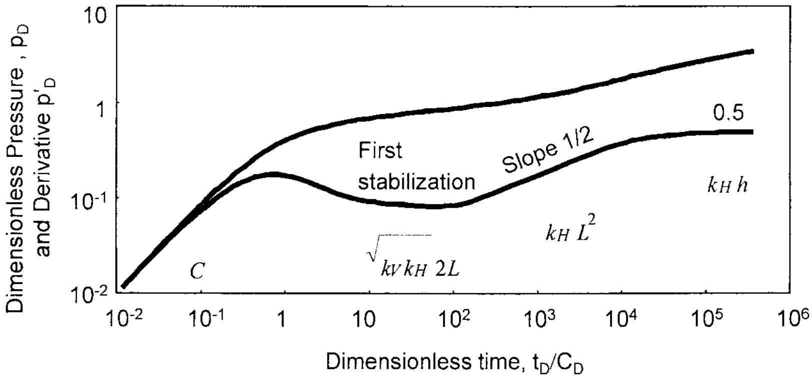

Figure 3.26. Horizontal well with wellbore storage and skin, homogeneous reservoir. Log-log scales, p_D versus t_D/C_D. C_D=1000, S_w =0, L =1000ft, h =100ft, r_w =0.25ft, z_w/h =0.5, k_V/k_H =0.1.

The basic horizontal well model is presented in details Sections 3.6.1 to 3.6.7. Variations from the ideal horizontal well geometry are discussed in Section 3.6.9, fractured and multilateral horizontal well responses are described in Sections 3.6.10 and 3.6.12. In Section 3.6.11, the influence of changes of reservoir properties in the horizontal or vertical directions, or change of fluid properties in the formation, are briefly reviewed. It is shown that when the basic horizontal well model depicted in Figure 3.24 is used to describe complex well or reservoir configurations, the effective well length and the average vertical permeability k_V resulting from analysis can be significantly in error. With complex wellbore conditions, k_V is frequently under-estimated whereas it can be over-estimated in layered systems with semi-permeable interbeds.

Analytical solutions

The first analytical solutions for uniform flux and infinite conductivity horizontal well responses have been derived in the mid 80's: Daviau et al. (1985), Clonts and Ramey (1986) and Rosa and Carvalho (1989) have used source and Green's functions whereas Goode and Thambynayagam (1987) and Kuchuk et al. (1991 a) obtained a solution by application of Laplace and Fourier transforms. With the infinite conductivity horizontal well model, the pressure is assumed constant along the wellbore. This is obtained by measuring the pressure of a uniform flux horizontal drain at an equivalent point in the well (Daviau, Clonts, Rosa), or by averaging the pressure along the length of the well (Goode, Kuchuk). The effect of pressure drop within the horizontal section, and the validity of the infinite conductivity assumption are discussed in Section 3.6.9.

Horizontal well solutions are approximate. They are generated using the line-source solution, which is valid only when $t_D / r_{wc}^2 > 25$. For large negative skin, this condition is not satisfied at early time. Furthermore, when the anisotropy between vertical and horizontal permeability is large, small discrepancies can be observed between different horizontal well solutions. With the uniform flux distribution, the pressure is not uniform around the wellbore circumference, and the choice of the reference point on the wellbore can influence the result slightly.

Dimensionless variables

For a horizontal well with wellbore storage and skin, the dimensionless variables are defined with respect to the total formation thickness. Equation 2.3 gives the dimensionless pressure.

In the case of permeability anisotropy between vertical and horizontal directions, an equivalent isotropic solution is used by introducing the anisotropy term k_V / k_H in the definition of the dimensionless vertical distances (see discussion of horizontal permeability anisotropy Section 3.1.5): when the vertical permeability k_V is low, the apparent vertical distances are increased. The apparent open interval thickness h_a and position of the horizontal drain hole with respect to the lower boundary of the zone z_{wa} are defined respectively :

$$h_a = h\sqrt{\frac{k_H}{k_V}} \tag{3.27}$$

$$z_{wa} = z_w\sqrt{\frac{k_H}{k_V}} \tag{3.28}$$

The circular section of the horizontal well is changed into an ellipse and the horizontal well behaves like a cylinder with the apparent larger equivalent radius r_{we} of Equation 3.6. With large anisotropy k_V / k_H , r_{we} can be 2 or 3 times larger than the actual wellbore radius and the resulting anisotropy skin S_{ani} clearly negative (see Table 3.1).

Several skin coefficients are defined for horizontal wells: the mechanical infinitesimal skin S_w, the anisotropy skin S_{ani}, the apparent skin during the vertical radial flow regime S_{TV}, the geometrical skin S_G and the total skin during the horizontal radial flow S_{TH}. The definitions of all skins are presented in detail in the subsequent sections.

In the definition of the dimensionless terms, several well parameters can be used for the reference length, considering the wellbore radius r_w or, by analogy with wells intercepting a fracture of half-length x_f (see Section 3.2, Equation 3.8), with the well half-length L. For the dimensionless time for example, t_D can be expressed by Equation 2.4 or by:

$$t_{DL} = \frac{0.000264k}{\phi\mu c_t L^2}\Delta t \tag{3.29}$$

No group of independent variables has been identified to provide a universal description of horizontal well responses, as it has been possible with most well models. Many authors use the ratio h_D of the apparent thickness h_a of Equation 3.27, by the well half length L, as a leading parameter of horizontal well behavior (similar to Equation 3.19):

$$h_D = \frac{h_a}{L} = \frac{h}{L}\sqrt{\frac{k_H}{k_V}} \tag{3.30}$$

In the following examples, the wellbore radius r_w is used in the dimensionless parameters definition. The dimensionless wellbore storage coefficient and the dimensionless time group t_D / C_D are given respectively in Equation 2.5 and 2.6. All examples presented below are generated with h = 100 ft and r_w = 0.25 ft and the dimensionless pressure p_D is presented versus the dimensionless time group t_D / C_D.

The question of the reference in the definition of the dimensionless terms is further discussed in subsequent sections for the different skin parameters estimated on horizontal well responses.

3.6.2 Equations for the characteristic regimes

In the following sections, the different limiting forms of the Kuchuk et al. (1991 a) solution are presented, and the different skin coefficients defined from horizontal well responses are described.

Radial flow in the vertical plane

During the vertical radial flow regime, the equation of the semi-log straight line is expressed (Kuchuk, 1995):

$$\Delta p = \frac{162.6qB\mu}{2\sqrt{k_V \cdot k_H}\, L}\left[\log\frac{\sqrt{k_V \cdot k_H}\,\Delta t}{\phi\mu c_t r_w^2} - 3.23 + 0.87S_w - 2\log\frac{1}{2}\left(\sqrt[4]{\frac{k_V}{k_H}} + \sqrt[4]{\frac{k_H}{k_V}}\right)\right] \tag{3.31}$$

The second logarithm of Equation 3.32 corresponds to the negative anisotropy skin S_{ani} resulting from the equivalent wellbore radius r_{we} of Equation 3.6. The total skin factor S_{TV} measured from the early time radial flow analysis combines the wellbore mechanical skin factor S_w and S_{ani}.

$$S_{TV} = S_w + S_{ani} = S_w - \ln\frac{\sqrt[4]{k_V/k_H} + \sqrt[4]{k_H/k_V}}{2} \tag{3.32}$$

In the following text, it is assumed that the wellbore mechanical skin factor S_w is uniform along the well length. The influence of non-uniform damage is discussed in Section 3.6.9.

Linear flow regime

During the linear flow regime, the pressure changes as the square root of the elapsed time:

$$\Delta p = \frac{8.128qB}{2Lh}\sqrt{\frac{\mu\Delta t}{\phi c_t k_H}} + \frac{141.2qB\mu}{2\sqrt{k_V \cdot k_H}\, L}S_w + \frac{141.2qB\mu}{k_H h}S_z \tag{3.33}$$

The first term of Equation 3.33 is similar to Equation 1.25 for a well intercepting a fully penetrating vertical fracture. With a horizontal well, the flow lines have to converge towards the well located at z_w in the formation thickness. This partial penetration effect produces a pressure drop, expressed with the skin S_z. During the linear flow regime, the two skin effects S_w and S_z are additive.

$$S_z = -1.151\sqrt{\frac{k_H}{k_V}}\frac{h}{L}\log\left[\frac{\pi r_w}{h}\left(1+\sqrt{\frac{k_V}{k_H}}\right)\sin\left(\frac{\pi z_w}{h}\right)\right] \tag{3.34}$$

Equation 3.34 is approximate and only valid when the length of the well is long compared to the apparent thickness (Equation 3.30, $h_D \le 2.5$).

Pseudo-radial flow from the reservoir

Using the well half-length L as the reference for semi-log analysis of horizontal radial flow, Kuchuk et al. define:

$$\Delta p = 162.6\frac{qB\mu}{k_H h}\left[\log\frac{k_H \Delta t}{\phi\mu c_t L^2} - 2.53\right] + \frac{141.2qB\mu}{2\sqrt{k_V k_H}\,L}S_w + \frac{141.2qB\mu}{k_H h}S_{zT} \tag{3.35}$$

where S_{zT} is :

$$S_{zT} = S_z - 0.5\frac{k_H}{k_V}\frac{h^2}{L^2}\left(\frac{1}{3} - \frac{z_w}{h} + \frac{z_w^2}{h^2}\right) \tag{3.36}$$

In practice, the efficiency of horizontal wells is frequently described by the total skin S_{TH} defined with reference to a fully penetrating vertical well of radius r_w. With the usual radial flow relationship,

$$\Delta p = 162.6\frac{qB\mu}{k_H h}\left[\log\frac{k_H \Delta t}{\phi\mu c_t r_w^2} - 3.23 + 0.87 S_{\mathrm{TH}}\right] \tag{3.37}$$

the total skin factor S_{TH} combines the wellbore mechanical skin factor S_w and the geometrical skin S_G. Comparing Equations 3.35 and 3.37,

$$\begin{aligned} S_{\mathrm{TH}} &= \frac{h}{2L}\sqrt{\frac{k_H}{k_V}}S_w + S_G \\ &= \frac{h}{2L}\sqrt{\frac{k_H}{k_V}}S_w + S_{zT} + 1.151\left(0.70 + 2\log\frac{r_w}{L}\right) \end{aligned} \tag{3.38}$$

the horizontal well geometrical skin S_G is expressed as :

$$S_G = 0.81 - \ln\frac{L}{r_w} + S_{zT}$$

$$= 0.81 - 1.151\left\{2\log\frac{L}{r_w} + \sqrt{\frac{k_H}{k_V}}\frac{h}{L}\log\left[\frac{\pi r_w}{h}\left(1+\sqrt{\frac{k_V}{k_H}}\right)\sin\left(\frac{\pi z_w}{h}\right)\right]\right\} \tag{3.39}$$

$$-0.5\frac{k_H}{k_V}\frac{h^2}{L^2}\left(\frac{1}{3}-\frac{z_w}{h}+\frac{z_w^2}{h^2}\right)$$

In Equation 3.39, the term $[0.81 - \ln(L/r_w)]$ is very close to the pseudo-skin of a fractured well (Equation 3.12) and S_{zT} (Equation 3.36) describes the pressure drop due to the convergence of the flow lines before reaching the well. This term disappears when h_D of Equation 3.30 is very small, for example in the case of a long well and high vertical permeability k_V. The geometrical skin S_G of horizontal wells is further discussed in Section 3.6.4.

3.6.3 Derivative behavior

Description

Due to the complex behavior of pressure and derivative responses, no type curves are available for horizontal wells. The derivative log-log curve is used for the identification of the characteristic flow regimes, but the analysis is made by generating pressure and derivative responses with a computer or, when applicable, by using specialized plot straight lines.

In the example of a horizontal well response of Figure 3.26, the last derivative stabilization (on the 0.5 line) corresponds to *pseudo radial flow* in the producing zone whereas the first stabilization describes the initial *radial flow in the vertical plane*. The average permeability in the vertical plane is defined as the geometric mean of k_V and k_H and the permeability thickness product is $2\sqrt{k_V \cdot k_H}\, L$. In dimensionless terms, the level of the first stabilization is expressed with the dimensionless apparent thickness h_D:

$$(\Delta p_{\text{1st stab.}})_D = 0.25 h_D = 0.25\frac{h}{L}\sqrt{\frac{k_H}{k_V}} \tag{3.40}$$

When both the upper and the lower boundary have been reached, there is no vertical contribution to the flow any more, and expansion of the drainage volume becomes strictly horizontal. If the length of the well is significantly larger than the reservoir thickness, most of the production is due to *linear flow* in front of the horizontal drain, and the flow contribution from the two ends of the well are negligible. During this intermediate time linear flow regime, the derivative follows a half-unit slope straight line.

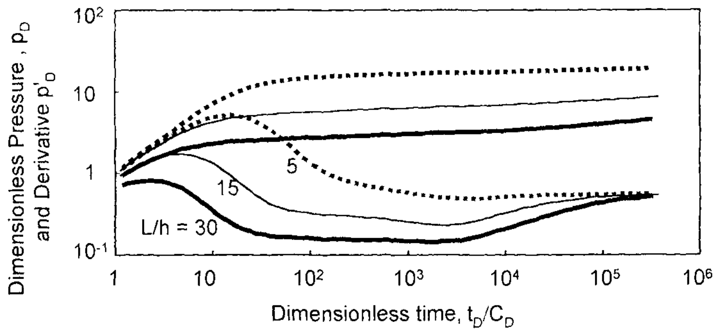

Figure 3.27. Horizontal well. Influence of L. Log-log scales, p_D versus t_D/C_D. C_D=1000, S_w=5, k_V/k_H=0.004, r_w=0.25ft, z_w/h=0.5, L=3000, 1500 and 500ft.

Once the linear flow regime has started, horizontal wells behave like wells intercepting an infinite conductivity vertical fracture of half-length $x_f = L$ (Section 3.2). The presence of an initial vertical radial flow regime before linear flow is simply seen as a skin on the equivalent fracture model (Equations 3.34 during linear flow and 3.39 during pseudo-radial flow).

Influence of L and k_V/k_H

With the t_D/C_D time scale, the location of the half unit slope straight line indicates the effective well half-length L. When L is doubled, the line is *displaced* by a factor of 4 along the time scale and, as the first derivative stabilization is an inverse function of L, $\Delta p_{1\text{st stab.}}$ is *twice as low* (Figure 3.27).

In the examples of Figures 3.28 and 3.29, three well lengths are considered but the permeability anisotropy k_V/k_H is adjusted in order to keep the same derivative stabilization during the vertical radial flow regime. With Figure 3.28, the vertical permeability k_V is relatively large and $(\Delta p_{1\text{st stab.}})_D = 0.223$ is below the radial flow 0.5 line. In such cases, the horizontal drain produces a *negative geometrical skin* (See discussion of the geometrical skin Sections 3.6.4 and 3.7).

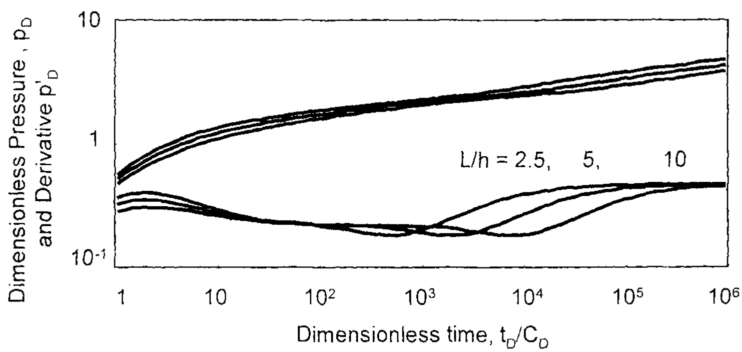

Figure 3.28. Horizontal well. Influence of L, $(\Delta p_{1\text{st stab}})_D$= 0.223. C_D=100, S_w=0, k_V/k_H=0.2, L=250ft; k_V/k_H=0.05, L=500ft; k_V/k_H=0.0125, L=1000ft; h=100ft, r_w=0.25ft, z_w/h=0.5.

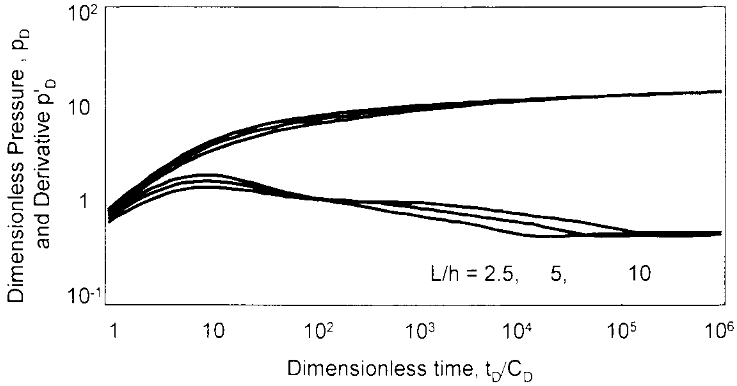

Figure 3.29. Horizontal well. Influence of L. $(\Delta p_{1st\ stab})_D = 1$. $C_D = 100$, $S_w = 0$, $k_V/k_H = 0.01$, $L = 250$ft; $k_V/k_H = 0.0025$, $L = 500$ft; $k_V/k_H = 0.000625$, v=1000ft; $h = 100$ft, $r_w = 0.25$ft, $z_w/h = 0.5$.

Conversely, when k_V is low, the first derivative stabilization is above 0.5 ($\left(\Delta p_{1st\ stab}\right)_D = 1$ on the examples Figure 3.29), and the horizontal well behavior tends to be equivalent to a well in partial penetration (Section 3.4). In the case of low vertical permeability, short horizontal wells exhibit a *positive geometrical skin*, and therefore an overall damaged well behavior. This is an important point and demonstrates that not all horizontal wells will increase productivity.

Influence of z_w/h

The first vertical radial flow lasts until one of the upper or the lower boundary is reached. If the horizontal well is not centered in the zone thickness ($z_w/h \neq 0.5$), *a hemi-radial flow* regime can develop when only the closest limit is seen. As long as the second sealing boundary is not reached, the shape of the derivative curve is similar to that of a vertical well near a sealing fault (Section 5.1). The second derivative stabilization is at a level twice the first (of Equation 3.40), as illustrated on the examples of Figure 3.30.

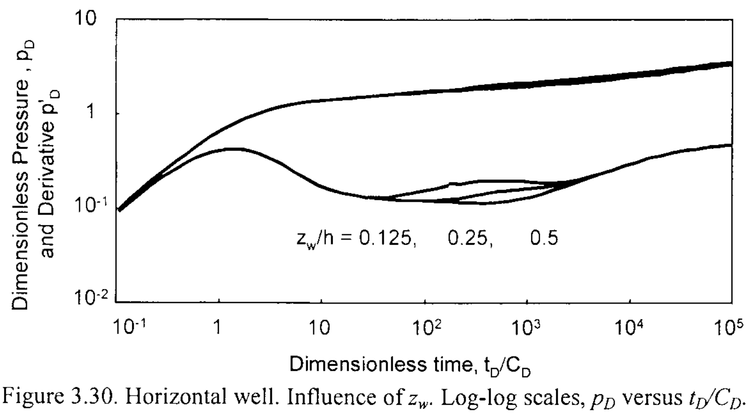

Figure 3.30. Horizontal well. Influence of z_w. Log-log scales, p_D versus t_D/C_D.
$C_D = 1000$, $S_w = 2$, $L = 1500$ft, $k_V/k_H = 0.02$, $h = 100$ft, $r_w = 0.25$ft, $z_w/h = 0.5$, 0.25, 0.125.

The influence of z_w/h on horizontal well responses is further discussed next and in Section 3.6.6, with a semi-log plot of Figure 3.30 examples.

3.6.4 Skin of horizontal wells

Since several distinct flow regimes are observed during horizontal well responses, several skin parameters can be defined to describe the different flow geometries, even though the infinitesimal skin damage S_w is constant at the wellbore. Furthermore, since the skin factors are a dimensionless pressure drop, several references can be used to normalize the different Δp_{skin}. In the following, we summarize the influence of the well and reservoir parameters on the three skins usually estimated from analysis. We show that, in the presentation of the analysis results, the reference used to express the skin parameters must be clearly defined.

Mechanical skin S_w

As an extension of the total horizontal radial flow skin concept S_{TH} used in Equation 3.37, the infinitesimal wellbore skin S_w is sometimes also defined with reference to a vertical well of radius r_w and a permeability k_H. The resulting skin parameter S'_w does not define the completion quality as does S_w of Equations 3.31 and 3.32.

$$S'_w = 0.5 h_D S_w = \frac{h}{2L}\sqrt{\frac{k_H}{k_V}} S_w \tag{3.41}$$

Geometrical skin S_G

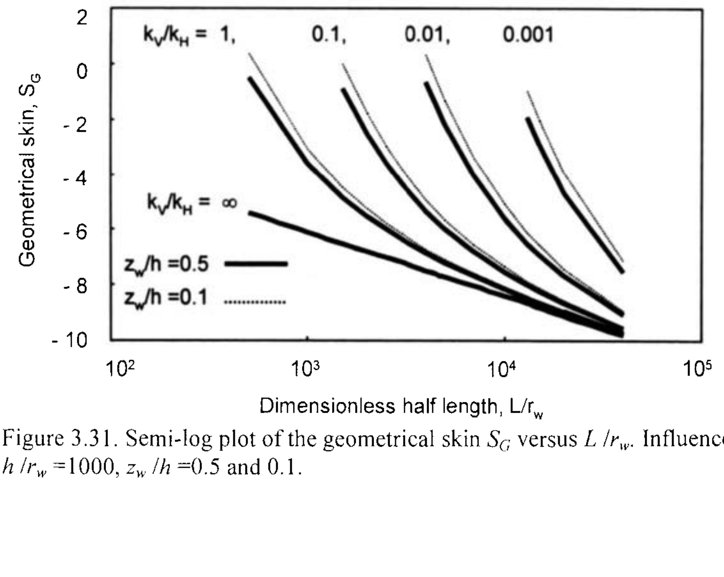

Figure 3.31. Semi-log plot of the geometrical skin S_G versus L/r_w. Influence of k_V/k_H. h/r_w =1000, z_w/h =0.5 and 0.1.

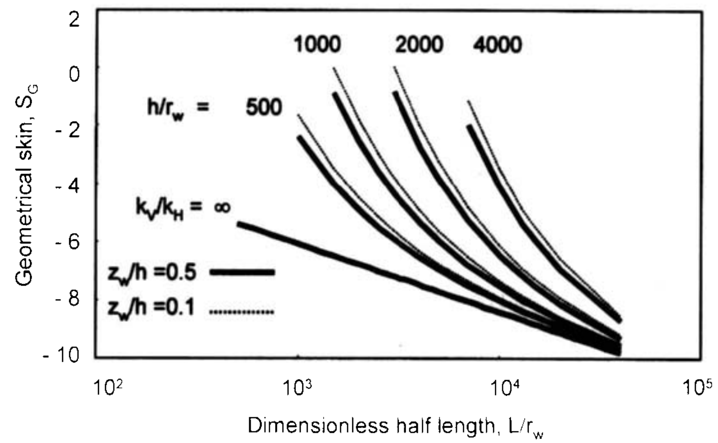

Figure 3.32. Semi-log plot of the geometrical skin S_G versus L/r_w. Influence of h/r_w. k_V/k_H =0.1, z_w/h =0.5 and 0.1.

On Figures 3.31 and 3.32, the geometrical skin S_G of Equation 3.39 is graphed versus $\log(L/r_w)$. With Figure 3.31, several hypothesis of permeability anisotropy k_V/k_H are considered, assuming a constant formation thickness h/r_w. When the vertical permeability is very large ($k_V \rightarrow \infty$), the *partial penetration* term S_{zT} cancels out, and the negative geometrical skin S_G is a linear function of $\log(L/r_w)$. When a vertical pressure drop is introduced as on the examples $k_V / k_H \leq 1$, the geometrical skin is less negative, and the curves reach the infinite vertical permeability behavior only when the drain hole is very long.

For a given permeability anisotropy k_V / k_H, increasing the formation thickness h/r_w also produces more partial penetration skin effect as shown on Figure 3.32. Again, when the horizontal well becomes very long, the adverse effect of the vertical pressure drops on the geometrical skin S_G is reduced. Ozkan and Raghavan (1989) indicate that the late time response of horizontal wells tends to be equivalent to that of vertically fractured ones when $h_D \leq 0.25$.

The dotted curves on Figures 3.31 and 3.32 show the geometrical skin when the well is not centered in the formation thickness. With z_w/h =0.1, a small additional pressure drop is introduced on the response, and S_G is slightly *less negative* (see discussion of Figure 3.33 in Section 3.6.6).

Total skin S_{TH}

As shown on Equation 3.38, the total skin S_{TH} estimated on horizontal well responses combines the geometrical skin S_G of Equation 3.39 and the mechanical infinitesimal skin S_w normalized by h_D (to give S'_w of Equation 3.41). For long horizontal drain holes, h_D is in general smaller than unity and the effect of a wellbore damage is *reduced.* The opposite effect is observed on partially penetrating wells, where a mechanical skin damage S_w is amplified in the total skin (Equation 3.17).

3.6.5 Matching procedure on pressure and derivative responses

Frequently, horizontal well responses do not exhibit the three individual flow regimes. Horizontal wells involve large wellbore volume, therefore a large wellbore storage coefficient and the wellbore storage effect lasts in general longer than in vertical wells. For this reason, the first radial flow may be difficult to identify. The last derivative stabilization is not always present within a normal test duration: the linear flow transition, before pseudo-radial flow regime, can last several log cycles on the time scale. The log-log diagnostic indicates the different flow regimes present on the response, and which parameters, or groups of parameters, can be estimated and which are not defined. Manual log-log analysis is not appropriate with horizontal wells, the match is performed on a computer-generated response.

When the complete sequence of flow regimes is identified on the derivative response, the early time *unit slope* straight line and the *final stabilization* are used to define the time and pressure matches, yielding the permeability-thickness product $k_H h$ from Equation 2.9 and the wellbore storage coefficient C from Equation 2.10. The intermediate time linear flow regime is used to estimate the effective well half-length L, by adjusting the match of the generated curve on the *half unit* slope straight line. k_H and L being defined, the *first derivative stabilization* determines the permeability anisotropy k_V / k_H. The match of the pressure curve during the initial vertical radial flow regime gives the mechanical skin S_w (or S_{TV}). The geometrical skin S_G, and therefore the total skin S_{TH} are defined from the estimated well and reservoir parameters (Equations 3.39). When the analysis is consistent, the theoretical pressure curve matches the data during the complete response.

Frequently, some segments of the well do not produce and the effective length $2L$ resulting from analysis is smaller than the drilled length. In Section 3.6.9, it is shown in the discussion of Figures 3.37 and 3.38 that, when several sections opened to the flow are distributed along the complete drain hole, a good match is frequently obtained by assuming the total drilled length. Then, the estimated vertical permeability k_V can be greatly *under estimated.*

When the vertical radial flow regime is masked by wellbore storage, the permeability anisotropy k_V / k_H cannot be assessed. The late time data give the total skin S_{TH} but, since the geometrical skin S_G is not defined, S_w is not reliable. Different hypothesis of k_V / k_H can change S_w from negative to positive values.

If the test data ends before the final derivative stabilization is reached, the horizontal permeability k_H and the total skin S_{TH} are not fixed, but the half unit slope straight line gives $k_H L^2$ (see Equation 3.33). In such case, the vertical permeability k_V can be estimated from the vertical radial flow derivative stabilization, if present. Again, the permeability anisotropy k_V / k_H and the mechanical skin S_w are not accurately defined, but the error on S_w is in general small.

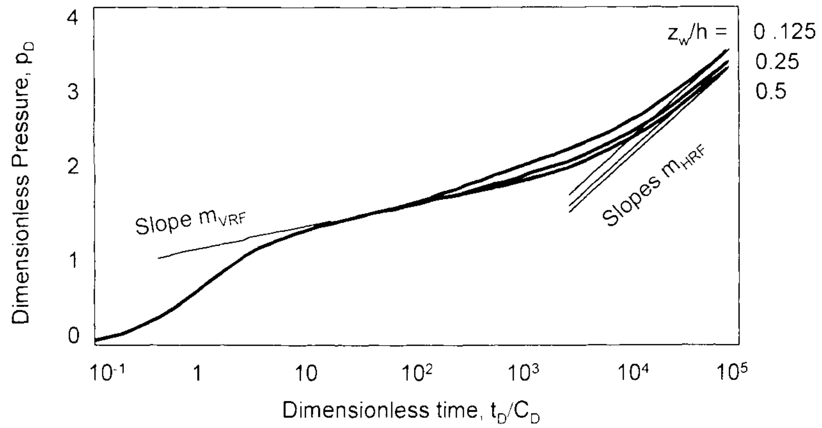

Figure 3.33. Semi-log plot of Figure 3.30 examples.

3.6.6 Associated specialized plot straight lines

Four specialized analyses are possible, depending upon the type and the duration of the regimes defined by the derivative log-log plot. The wellbore storage analysis is the same as for vertical wells (Section 1.3.2). In the following section, straight-line analysis methods are presented for the vertical radial flow, linear flow and the horizontal pseudo radial flow regimes.

Figure 3.33 is a semi-log plot of the Figure 3.30 examples for three different well locations z_w/h. When the well is centered (z_w/h =0.5), the response exhibits two straight lines on semi-log scale and, as the permeability thickness product during the initial vertical radial flow is larger than $k_H\, h$, the first slope m_{VRF} is lower than the final straight line slope m_{HRF}. When the well is off-centered, an intermediate time straight line of slope 2 m_{VRF} can be observed during the hemi-radial flow in the vertical plane (curve z_w/h =0.125). In such case, the final semi-log straight line is displaced upwards, because of the influence of z_w/h on the geometrical skin S_G of Equation 3.39. A similar effect on late time semi-log straight lines can be observed in reservoirs with multiple boundaries (Figure 5.13 of Chapter 5 for example).

Frequently, after wellbore storage, horizontal well responses only show transitional behaviors between the characteristic flow regimes, and no specialized analysis is possible. Furthermore, with build-up data, the Horner or multiple-rate superposition methods used on the specialized plots can distort the characteristic straight lines, as a result of the changes of flow behavior during the response (see Section 2.3.4). Except for the final horizontal radial flow regime, the straight-line methods presented in the following are seldom used.

Radial flow in the vertical plane

During the first radial flow regime in the vertical plane, the equation of the semi-log straight line is expressed in Equation 3.31. The slope m_{VRF} gives the product of average permeability in the vertical plane $\sqrt{k_H k_V}$, multiplied by the perforated half-length L:

$$\sqrt{k_V k_H}\,L = \frac{81.3 qB\mu}{m_{\mathrm{VRF}}} \tag{3.42}$$

When L and the permeability anisotropy k_V/k_H are known, the skin S_{TV} measured from the first semi-log straight line is used to estimate the infinitesimal skin S_w. From Equation 3.31,

$$S_w = 1.151\left[\frac{p(1\mathrm{hr}) - p(\Delta t = 0)}{m_{\mathrm{VRF}}} - \log\frac{\sqrt{k_V k_H}}{\phi\mu c_t r_w^2} + 2\log\frac{1}{2}\left(\sqrt[4]{\frac{k_V}{k_H}} + \sqrt[4]{\frac{k_H}{k_V}}\right) + 3.23\right] \tag{3.43}$$

Provided the $\sqrt{k_H k_V}\,L$ product is correctly estimated from m_{VRF}, the dependence of S_w on the anisotropy k_V/k_H and on the effective well half-length L are logarithmic. The calculation of the infinitesimal skin with Equation 3.43 is not very sensitive to an error on k_V/k_H or L (in Section 3.1.5, it is shown that S_{ani} is in general between 0 and -1).

When the nearest upper or lower sealing boundary is reached, the flow regime changes to hemi-radial flow and the response deviates from the semi-log slope m_{VRF} to follow a semi-log straight line of slope $2m_{\mathrm{VRF}}$. The time of intercept between the m_{VRF} and $2m_{\mathrm{VRF}}$ straight lines can be used to estimate the vertical permeability k_V with a relationship similar to Equation 1.33 for a sealing fault (see section 5.1.3). Kuchuk et al. (1991 a) propose to use the time Δt_{end} of end of the initial vertical radial flow (i.e. when the derivative deviates from the first stabilization, and not the mid point of the derivative transition as in section 5.1.1) with :

$$k_V = \frac{\phi\mu c_t}{0.000264\pi\Delta t_{end}}\min\left\{z_w^2, (h - z_w)^2\right\} \tag{3.44}$$

For a build-up analysis, the first straight line extrapolated pressure is not used, p^* is estimated from the horizontal radial flow regime (Section 3.6.7).

Linear flow regime

This flow regime results of the influence of the two sealing upper and lower limits. As already mentioned, the horizontal well behaves like an infinite conductivity fractured well, but the linear flow regime can also be described as a boundary effect. In fact, by rotating the horizontal well through 90°, the configuration is similar to a vertical well between two parallel sealing faults (Chapter 5.2). As opposed to a fractured well and channel responses, described by Figures 3.5 and 5.4 for example, none of the curves presented in Figures 3.26 to 3.30 present a long derivative half unit slope straight line. On horizontal well responses, the vertical radial and hemi-radial flow regimes dominate the early time data. Later, the transition between linear flow and the final pseudo radial flow regime is long, a flow contribution from the reservoir region at both ends of the well is felt a long time before the start of the final radial flow regime, and the pure linear flow regime is short lived. In order to see this characteristic regime, the distance between the two derivative stabilizations must be large. From Equation 3.40, it can be seen that the well length $2L$ must be very long compared to the apparent thickness h_a of Equation 3.27 (small h_D, Kuchuk et al., 1990).

When the half unit slope derivative straight line is clearly established, the corresponding pressure points are analyzed on a plot of the pressure versus the square root of the elapsed time, as for a fractured well or a channel reservoir (see Sections 3.2 and 5.2). From Equation 3.33, the slope m_{LF} of the straight line gives $k_H L^2$:

$$k_H L^2 = 16.52\left(\frac{qB}{m_{LF}\,h}\right)^2 \frac{\mu}{\phi c_t} \tag{3.45}$$

The intercept p(0hr) of the linear flow straight line at time 0 can theoretically be used to estimate the infinitesimal skin S_w (Kuchuk et al., 1990):

$$S_w = \frac{2\sqrt{k_V \cdot k_H}\,L}{141.2qB\mu}\left[p(0hr) - p(\Delta t = 0)\right] + 2.303\log\left[\frac{\pi r_w}{h}\left(1 + \sqrt{\frac{k_V}{k_H}}\right)\sin\left(\frac{\pi z_w}{h}\right)\right] \tag{3.46}$$

Alternatively, when S_w is known from previous vertical radial flow regime, z_w/h can be estimated from Equation 3.46 in the same way as, for channel reservoirs, the intercept p(0hr) defines the well location between the faults (see Section 5.2.5). It can be noted that the linear flow partial penetration skin effect S_z of Equation 3.34 has the same form as the geometrical skin of channel reservoir (Equation 5.8), discussed in Section 5.2.5.

Pseudo-radial flow from the reservoir

The analysis of the pseudo-radial flow regime is identical to the semi-log analysis of a vertical well response (Equation 3.37). The straight line slope m_{HRF} gives the horizontal permeability thickness product $k_H\,h$, the straight line intercept at 1 hour is used to estimate the total skin coefficient S_{TH} and, for a build-up periods, the extrapolation to infinite shut-in time gives p^*.

$$k_H h = \frac{162.6qB\mu}{m_{HRF}} \tag{3.47}$$

$$S_{\mathrm{TH}} = 1.151\left[\frac{p(1\mathrm{hr}) - p(\Delta t = 0)}{m_{\mathrm{HRF}}} - \log\frac{k_H}{\phi\mu c_t r_w^2} + 3.23\right] \tag{3.48}$$

Either the mechanical skin S_w or the geometrical skin S_G can be estimated from Equations 3.38 and 3.39.

3.6.7 Build-up analysis

On horizontal well responses, the flow geometry changes from early time to late time and three different characteristic regimes can be observed, as illustrated on previous derivative examples. For shut-in periods, the Horner and time superposition methods used for straight line and derivative analysis are based on the assumption that all superposed periods follow the same flow regime (see Section 2.2.2 and 2.3.4). In the case of complex responses, it is likely that the extrapolated periods follow different behaviors, and the multiple-rate superposition method is theoretically invalid.

The resulting build-up derivative can be distorted (see discussion Figure 2.20 for example) but, since the log-log match of horizontal well responses is made on a computer generated multiple-rate pressure and derivative curves, the use of superposition time does not introduce error in the results.

With straight-line methods, it is found in practice that unless the production time is very short and the well has been closed during the vertical radial flow regime, the superposition methods are applicable for all flow regimes.

The semi-log superposition function can be used for radial flow analysis. As the producing time t_p is generally significantly greater than Δt during the early time vertical radial flow regime, the Horner time can be simplified with $\log(t_p + \Delta t/\Delta t) \approx \log t_p - \log \Delta t$ (Equation 2.16), and the result becomes independent of the production history. On a Horner plot of horizontal well response, the first straight line gives the correct $\sqrt{k_H k_V}\,L$ product with Equation 3.42. The first straight line extrapolated pressure is not used, the pressure at infinite shut-in time p^* is estimated from the second straight line during the horizontal radial flow regime, if present.

When the linear flow regime is clearly established, build-up responses can be analyzed with the Horner or multiple-rate superposition time corresponding to this flow regime (Equation 2.19). If the previous drawdown had reached the horizontal pseudo radial flow at time of shut-in, $t_p >> \Delta t$ then the method remains applicable.

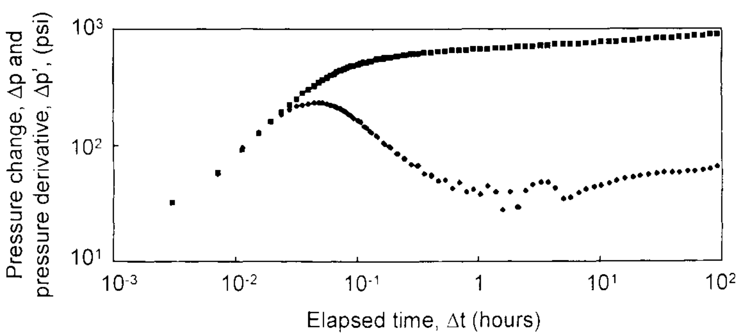

Figure 3.34. Build-up test in a horizontal well. Log-log scales.

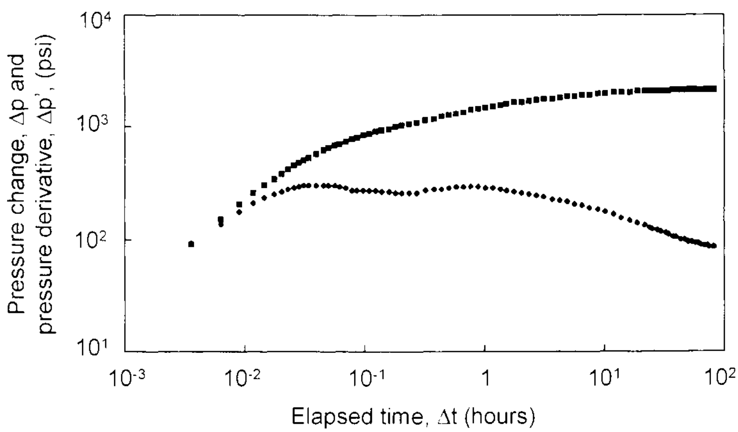

Figure 3.35. Build-up test in a horizontal well. Log-log scales.

3.6.8 Field examples

In Figures 3.34 and 3.35, two examples of horizontal well build-up tests are presented. For the example in Figure 3.34, the response describes the wellbore storage unit slope straight-line, followed successively by the characteristic derivative hump, a first derivative stabilization during the vertical radial flow, an increase of derivative near 10 hours, and the final derivative stabilization during the horizontal radial flow. This well shows a usual horizontal well behavior similar to the responses in Figure 3.26, *all reservoir and well parameters* can be estimated. The geometrical skin of this horizontal well is *negative*.

A completely different response is obtained on the 100 hours build-up example of Figure 3.35. After a short wellbore storage effect, the derivative stabilizes during the first hour, and later it declines slowly until the end of the build-up test. No final derivative stabilization is seen; the horizontal radial flow is not reached. The overall behavior is similar to the low k_V examples of Figure 3.29: the geometrical skin is *positive*. Straight-line analysis of this horizontal well response is only applicable during the *vertical radial flow* regime, to provide $\sqrt{k_H k_V}\,L$ and S_w. When the data is matched against a computer-generated model, a relatively unique analysis is obtained. The mechanical skin S_w is negative (no derivative hump is seen before the stabilization).

3.6.9 Discussion of the horizontal well model

In the following, several variations of the basic horizontal well model are considered. With finite conductivity wells, or when the skin is non-uniform along the well length, and with partially open horizontal wells, a pressure gradient is introduced in the reservoir along the well length. These wellbore conditions can distort the pressure response, especially at early time, and produce an under estimated $\sqrt{k_V k_H}\,L$ product when they are ignored. In case of non-rectilinear wells, the response is affected at intermediate times, with little effect one the estimated parameters.

Finite conductivity horizontal wells

In the previous discussion, the horizontal drain is assumed to be of infinite conductivity. Frequently, highly productive horizontal wells are completed with small diameters and the pressure gradients along the well length cannot be neglected, particularly when the flow becomes turbulent. Several authors have considered the effect of pressure drop in the wellbore on horizontal well responses (Dikken, 1990; Ozkan et al., 1995; Ozkan and Raghavan, 1997).

Using the same approach as Cinco et al. (1978 a) for finite conductivity fractured wells, Ozkan et al. express the pressure drop with an equivalent wellbore permeability in the case of laminar flow. The conductivity of the horizontal well is defined as an inverse function of the well length $2L$. They describe the flux distribution along the wellbore as follows, for high and low conductivity wells:

- When the pressure gradients in the wellbore are negligible compared to the pressure gradients in the reservoir, the well shows a high conductivity behavior. At early time, the flux distribution is uniform along the wellbore. When the flow tends towards the horizontal radial flow regime, the *two ends* of the horizontal drain are the most productive sections, and the flux profile along the well length is described by a U-shaped symmetric distribution, similar to the flux towards a well with an infinite conductivity fracture (Figure 3.13).
- In the case of a low drawdown (such as when the reservoir permeability is high, the thickness small and the horizontal section long), when the wellbore radius is not large enough, the pressure drop in the wellbore can be comparable to the pressure drop in the reservoir. The well behavior deviates from the infinite conductivity response. Due to the pressure gradients in the low conductivity well, most of the fluid enters near the *heel of the well*, resulting in a distortion of the flux profile from the uniform or U-shaped distribution, into an asymmetric shape.

As for the finite conductivity fracture model of Cinco et al., the effect of a finite conductivity horizontal well is more pronounced at early times. The presence of high pressure gradients in the wellbore can distort the pressure response during the vertical radial flow and linear flow regimes, since the flow in the reservoir becomes *three dimensional* (with a component parallel to the well axis). For low conductivity horizontal wells, the derivative is above the vertical radial flow stabilization of Equation 3.40. The effect of wellbore friction is the highest in non-damaged horizontal wells, and it tends to be reduced when the mechanical skin factor S_w is large (Ozkan and Raghavan, 1997).

By neglecting wellbore hydraulics, the product $2\sqrt{k_V \cdot k_H}\,L$ can be underestimated by a factor of 3 or more, but the permeability-thickness product $k_H\,h$ should be accurately defined. In the analysis results, both the vertical permeability k_V and the effective well half-length L are too low, whereas the estimated mechanical skin factor S_w is too large.

During the horizontal radial flow regime, the authors explain that the wellbore pressure gradients simply introduce an additional pressure drop and the response of a low conductivity horizontal well becomes similar to that of a *damaged infinite conductivity* horizontal well (with a less negative total skin S_{TH}).

Bourgeois et al. (1996 a) propose to approximate the effect of wellbore friction on the total skin S_{TH} by a rate dependent skin effect similar to the non-Darcy skin of gas wells (Section 7.2.4). The total skin of Equation 3.38 is then changed into :

$$S_{TH} = \frac{h}{2L}\sqrt{\frac{k_H}{k_V}}\left(S_w + Dq\right) + S_G \tag{3.49}$$

where Dq describes the friction skin during the horizontal radial flow regime.

Non-uniform mechanical skin

Ozkan and Raghavan (1997) investigated the influence of a non-uniform mechanical skin on infinite conductivity horizontal well responses. They concluded that, in early time response, a change of skin damage along the well length tends to move the derivative above the vertical radial flow stabilization of Equation 3.40. During the horizontal radial flow regime, the derivative stabilization can be used to estimate the $k_H h$ product but the well productivity (or the total skin S_{TH}) is slightly influenced by the skin factor distribution. S_{TH} is more negative when the two ends of the horizontal drain are not damaged, and the mechanical skin is mostly located in the central section of the well. No damage at the *heel and toe* of the well improves the productivity because of the U-shaped flux profile discussed earlier for high conductivity horizontal drains. As described next, a similar conclusion is obtained with partially completed horizontal wells.

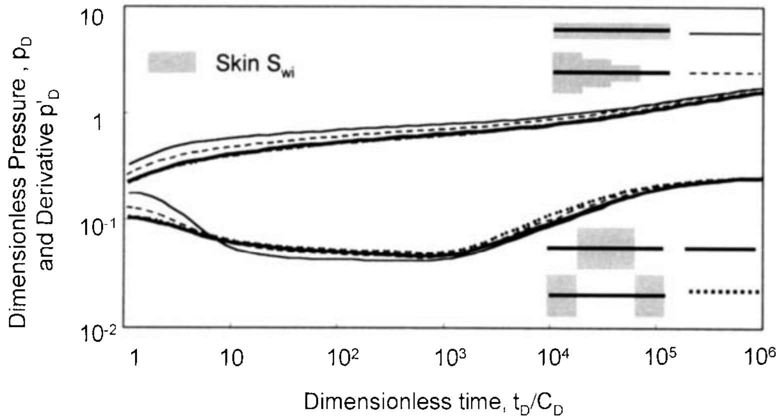

Figure 3.36. Horizontal well. Influence of non-uniform skin. Log-log scales, p_D versus t_D/C_D. C_D =100, L =1000ft, h =100ft, r_w =0.25ft, z_w / h =0.5, k_V / k_H =0.1. Four segments L_{wi}= L /4 with S_{wi} =(4 - 4 - 4 - 4), (8 - 5.3 - 2.6 - 0), (0 - 8 - 8 - 0), (8 - 0 - 0 - 8).

On Figure 3.36, three examples of non-uniform skin distributions are compared to the response of a well with a constant mechanical skin factor S_w = 4. The well length is divided into four equal segments and each segment is affected by a skin factor S_{wi} such as the arithmetic mean of S_{wi} is constant at 4. In one case, the skin is linearly decreasing from one end to the other and, in the two other cases, the damage is either located on the two external segments or on the central sections. The examples Figure 3.36 confirms that, when the ends are not damaged, the total skin of the well S_{TH} is slightly more negative than on the three other responses (S_{TH} = -6.4 instead of -6.2). The authors conclude that stimulation treatments of horizontal wells should preferably concentrate on the *heel and the toe*.

Partially open horizontal wells

Frequently, some sections of the horizontal drain are not contributing to the flow and the effective well half-length L estimated by analysis is smaller than the length of the drilled well. It is shown in the following that the pressure behavior of partially open horizontal wells depends not only upon the effective well half-length L, but also upon the number and the distribution of the open sections along the well-drilled length (Goode and Wilkinson, 1991; Kamal et al., 1993; Yildiz and Ozkan, 1994).

On Figure 3.37, three different repartition examples of the productive segments are compared. For all completion scenarios, the same effective well half-length is assumed with L_{eff}=1/4L of the total drilled length (the response corresponding to the fully open horizontal well is shown with the thin dotted curves). When only one section is producing, the response corresponds to a horizontal well with half-length L_{eff} (thin solid curves).

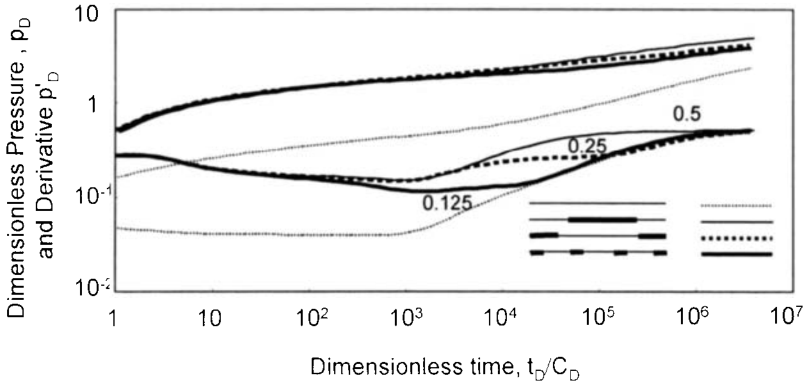

Figure 3.37. Partially open horizontal well. Influence of the number of open segments. C_D =100, 1, 2, 4 segments with S_{wi} =0. ΣL_{eff}= L /4. L =2000ft. h =100ft. r_w =0.25ft. z_w / h =0.5, k_V/k_H =0.1.

Whatever is the repartition of the open sections, only the total length of the producing intervals influences the response during the initial vertical radial flow. At early time, the pressure and derivative curves generated for several producing intervals shows the same behavior as the single producing interval with similar L_{eff}. Later, when the distances between the open intervals are large, each segment acts as a horizontal well, and a horizontal radial flow geometry develops around the different producing sections. Kamal et al. (1993) showed that, during this intermediate time radial flow regime, the derivative stabilizes at 0.5 divided by the number of open segments. When only the heel and toe of the well are producing (thick dashed pressure and derivative curves), the derivative stabilizes at 0.25 and, when four segments are open to flow, it stabilizes at 0.125 (thick solid curves).

Once the interference effect of neighboring segments is felt, the intermediate radial flow regime changes into linear flow and the derivative response reaches that of a single horizontal drain hole whose length corresponds to the *distance between the two ends* of the external open segments. During the final horizontal radial flow, the total skin S_{TH} is slightly more negative when the open section is more *distributed*: with 4 segments, S_{TH}= -6.7 on Figure 3.37 whereas S_{TH} = -6.3 in case of two segments and S_{TH} = -5.4 with only one segment.

When analyzing the example with four segments of Figure 3.37, the horizontal permeability is defined from the final derivative stabilization. The half unit slope derivative straight line gives access to maximum external distance of the open segments, which is 4 times the effective well length in this example. By assuming that 100% of the well length is producing with a single horizontal drain model, Kamal et al. (1993) noted that the vertical permeability value resulting from the vertical radial flow analysis of the first derivative stabilization is *under estimated* (by a factor of 16 in the example).

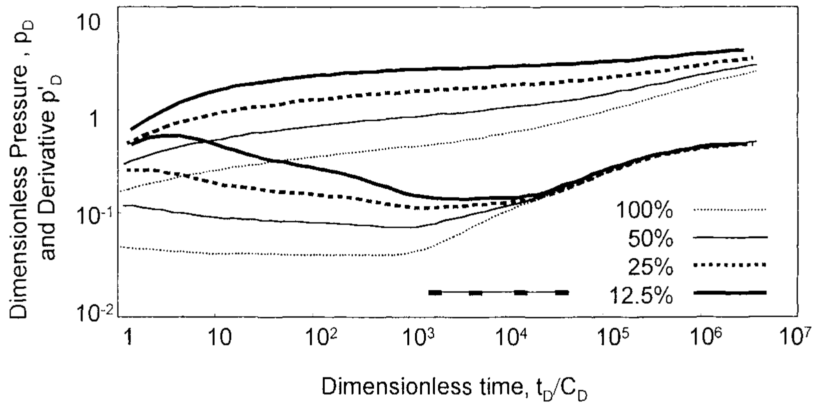

Figure 3.38. Partially open horizontal well. Influence of the penetration ratio. Log-log scales, p_D versus t_D/C_D. C_D =100, 4 segments with S_{wi} =0, ΣL_{eff}= L /8, L /4, L /2 and L, L =2000ft, h =100ft, r_w =0.25ft, z_w /h =0.5, k_V /k_H =0.1.

Figure 3.38 shows the influence of the penetration ratio for a horizontal well with four uniformly distributed segments of equal length. The ratio of the total length of the open segments to the length of the drilled well is respectively 12.5, 25, 50 and 100%. As already observed on Figure 3.37, all derivative curves merge at late time, during linear and pseudo radial flow, on the fully penetrating horizontal well response. Before, the derivative is displaced upwards. In case of low penetration ratio such as on the example 12.5%, the flow is *three-dimensional* at early time (Yildiz and Ozkan, 1994) with a decreasing derivative trend. Assuming no mechanical skin damage, the total skin S_{TH} of the fully penetrating horizontal well of Figure 3.38 is S_{TH} =-7.9. With a penetration ratio of 50, 25 and 12.5%, S_{TH} is still very negative with respectively –7.4, -6.6 and –5.1.

Yildiz and Ozkan (1994) presented a general selectively completed infinite conductivity horizontal well model. They observed that the rate profile and the pressure response are affected at early time by a non-uniform skin distribution between the productive segments and use of vertical radial flow analysis is not possible. They concluded that it is not possible to estimate length and distribution of the open interval from use of transient analysis.

Non-rectilinear horizontal wells

Horizontal wells are in general not parallel to the top and bottom sealing interfaces. In Figure 3.39, two examples of non-rectilinear horizontal well responses are compared to the straight horizontal drain hole model. Two symmetric geometries are considered: half of the well length is either centered in the formation thickness (z_w =0.5h) or close to upper or lower sealing boundary (z_w =0.05h). The other half, distributed in two equal segments at the heel and toe, is close to a boundary in the first case (z_w =0.05h), and centered in the other. The linear horizontal well, shown with a thin pressure and derivative curve, is located at the average distance with z_w =0.275h.

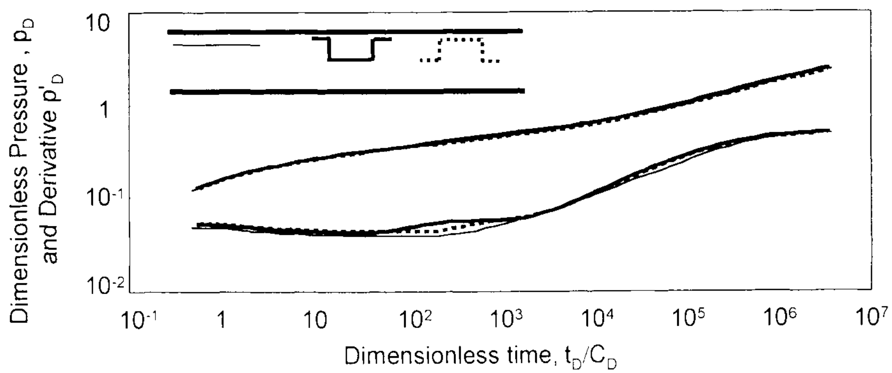

Figure 3.39. Non-rectilinear horizontal well. Log-log scales, p_D versus t_D/C_D. C_D =100, L =2000ft (500+1000+500), S_{wl} =0, h =100ft, r_w =0.25ft, k_V / k_H =0.1, $(z_w / h)_i$=0.5 or 0.95 (average 0.725).

When some segments of the horizontal well are closer to the upper or lower boundary, the vertical radial flow regime ends earlier than when the well is a single linear segment at the average vertical distance. The *transition* from the first derivative stabilization to the half unit slope straight line is slightly distorted but, as shown Figure 3.39, the three derivative responses are very similar. The pressure curves are not distinguishable (the total skin S_{TH} being slightly less negative when the two ends of the well are off-centered).

3.6.10 Fractured horizontal wells

When fracturing horizontal wells, the fracture direction with respect to the wellbore depends upon the orientation of the well compared to the least principal stress. If the well is drilled in the direction of the least stress, several vertical fractures transverse to the well may be created along the well length. When the well is perpendicular to the least stress, the fractures are parallel to the well.

Soliman et al. (1990) presented an approximate analytical solution for horizontal wells in the direction of the least stress, with circular finite conductivity transverse fractures. Larsen and Hegre (1991) investigated both circular transverse, and rectangular longitudinal, finite conductivity fractures. They assume the horizontal wellbore is not perforated outside the fractured segments.

With a transverse fracture, the flow at early time is linear from the formation to the fracture, and radial inside the fracture to the wellbore. Larsen and Hegre (1994 a) note that this *radial-linear flow* geometry is similar to that of transient double porosity reservoirs, slab matrix blocks with a semi-log straight line of slope half that of the radial flow in the fissure system (Section 4.1.3). With transverse fractures, the radial-linear flow regime is characterized by a semi-log straight line of slope m_{RLF} half that of the pure radial flow in the fracture. Therefore, the slope is only a function of the fracture conductivity $k_f w_f$:

$$m_{\mathrm{RLF}} = 81.3 \frac{qB\mu}{k_f w_f} \tag{3.50}$$

With a longitudinal fracture, a *bilinear flow* regime develops at early time, as for a vertical well intercepting a finite conductivity fracture. On a pressure versus $\sqrt[4]{\Delta t}$ plot, the slope m_{BLF}, similar to Equation 1.27, is a function of the fracture half-length x_f along the horizontal well direction. When the reservoir permeability k_H is known, m_{BLF} also gives access to the fracture conductivity $k_f w_f$:

$$m_{\mathrm{BLF}} = 44.11 \frac{qB\mu}{x_f \sqrt{k_f w_f} \sqrt[4]{\phi \mu c_t k_H}} \tag{3.51}$$

In the case of a single fracture, the radial-linear or bilinear flow regime is followed by the *formation linear flow*, and finally the pseudo-radial flow towards the horizontal well. During the linear flow regime, the slope m_{LF} of the pressure versus $\sqrt{\Delta t}$ straight line can be used to estimate the fracture extension if the formation permeability is known. For a transverse circular fracture of radius r_f, the authors express m_{LF} as:

$$m_{\mathrm{LF}} = 5.17 \frac{qB}{hr_f} \sqrt{\frac{\mu}{\phi c_t k_H}} \tag{3.52}$$

For a rectangular fracture of horizontal extension $2x_f$, a relationship similar to Equation 3.45 is obtained:

$$m_{\mathrm{LF}} = 4.06 \frac{qB}{hx_f} \sqrt{\frac{\mu}{\phi c_t k_H}} \tag{3.53}$$

On a log-log derivative plot, the sequence of characteristic straight lines is, after wellbore storage,

1. *first stabilization* in case of transverse fracture (radial-linear flow) or *quarter unit slope* with longitudinal fracture (bilinear flow),
2. *half unit slope* during formation linear flow
3. *final stabilization* during formation pseudo radial flow.

The fracture conductivity determines the location of the first derivative straight line (stabilization or 1/4 slope). For high conductivity fractures, the derivative response is low during the radial-linear or bilinear flow regimes, the corresponding early time straight line is moved down on the log-log scale, and the formation linear flow develops early. It is shown in Section 3.6.3 that for non-fractured horizontal wells, the linear flow 1/2 slope defines the effective well length. In the case of fractured horizontal wells, it gives the *horizontal extension* of the fracture. With long fractures, the 1/2 slope derivative straight line is displaced towards late times.

For multi-fractured horizontal wells, the different fractures produce independently until interference effects between neighboring fractures are felt. Then, a compound linear flow develops before the final pseudo radial flow regime.

At early time, if the independent fractures have similar characteristics, the response is directly proportional to the number of fractures and can be analyzed with a single fracture model by dividing the flow rate by the number of fractures (Larsen and Hegre, 1994 a; Raghavan et al., 1997). Radial-linear (transverse fractures) or bilinear flow regimes (longitudinal fractures) can be analyzed on such multi-fractured horizontal well responses. Later, linear flow and pseudo radial flow around the different fracture segments (when the distance between the fractures is large) can also be identified. Once the interference between the fractures is felt, the response deviates like in the case of partially open horizontal wells presented in Section 3.6.9. The end of the compound linear flow regime, and start of the final pseudo radial flow, is independent of the number of fractures but depends only on the distance between the outermost fractures.

3.6.11 Horizontal wells in reservoirs with changes of permeability

In the following, it is shown that two types of reservoir heterogeneities affect the analysis results of horizontal well responses, even though the overall well behavior is apparently homogeneous. The influence of horizontal permeability anisotropy is first discussed. In layered reservoir, changes of permeability in the vertical direction can reduce the ability of vertical flow during the early time response.

Horizontal permeability anisotropy

With horizontal wells, it takes frequently a long time before the final horizontal radial flow regime is established. In the case of horizontal permeability anisotropy, the well response is sensitive to the well orientation (Goode and Thambynayagam, 1987; Kamal et al., 1993).

With the three directions of permeability defined on Figure 3.40, the characteristic regimes of an horizontal well response are controlled by a different permeability:

1. At early time, the average permeability during the vertical radial flow is $\sqrt{k_z k_y}$.
2. During the linear flow regime, only the permeability k_y normal the well orientation is acting.
3. The final horizontal radial flow regime defines the average horizontal permeability $\bar{k}_H = \sqrt{k_x k_y}$ of Equation 3.3.

When the isotropic horizontal permeability model is used for analysis, the vertical permeability k_z is unchanged but the apparent effective half-length is:

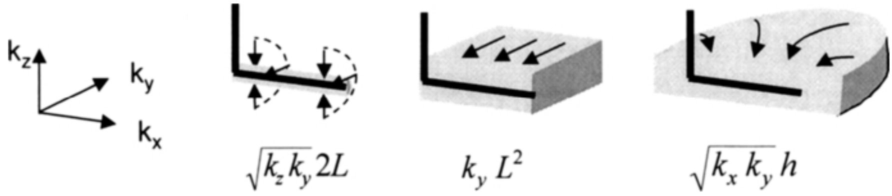

Figure 3.40. Horizontal permeability anisotropy.
Effective permeability during the three characteristic flow regimes towards a horizontal well.

$$L_a = \sqrt[4]{k_y / k_x}\, L \tag{3.54}$$

Equation 3.54 shows that, if the horizontal well is in the *minimum* (maximum) permeability direction, apparent effective length *increased* (decreased).

Horizontal wells in vertically heterogeneous reservoirs

Even though the homogeneous reservoir model is currently used for many well test analysis, most reservoirs are stratified and permeability varies with depth. In most cases, variations of horizontal permeability with depth do not alter significantly the horizontal radial flow regime (see Section 4.2) but, as horizontal wells responses are also sensitive to vertical flow, the changes of vertical permeability over the producing thickness affect the response.

In the following, the horizontal well model of Kuchuk and Habashy (1996) for a multi-layer reservoir with crossflow is used to evaluate the effect of vertical changes of k_V. It is shown that when the heterogeneity between the different layers is moderate, the homogeneous reservoir model can be used to provide average permeability in both horizontal and vertical directions. Conversely, when horizontal wells are completed in formations with several interbeds of reduced permeability between the main layers, the single homogeneous layer model considered in the previous sections is not appropriate for accurate analysis (Suzuki and Nanba, 1991). Finally, as horizontal drilling is a common practice in reservoirs with a gas cap or lower water drive to prevent coning or cresting, the effect of a constant pressure upper or lower boundary is discussed.

On the example Figure 3.41, the reservoir is described as a three-layer system. The horizontal well is centered in layer 2, layers properties are defined in Table 3.6.

Table 3.6. Layered system of Figure 3.41

Layer	h_i	k_{Hi}	k_{Vi}	$(k_V / k_H)_i$
1	30	15	1.2	0.08
2	30	10	0.5	0.05
3	40	8	0.24	0.03

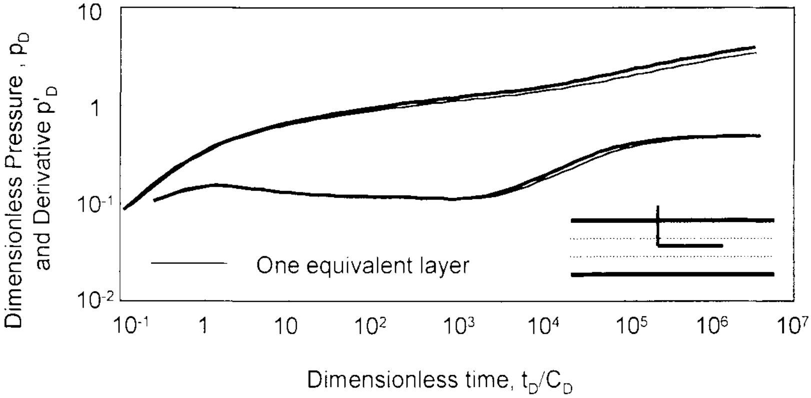

Figure 3.41. Horizontal well in a three layers reservoir with crossflow. Log-log scales, p_D versus $t_D C_D$. C_D =100. L =1000ft. S_w =0. h =100ft (30+30+40). r_w =0.25ft. z_w/h =0.55. k_{H1}/k_{H2}=1.5, k_{H3}/k_{H2}=0.8. $(k_V/k_H)_1$=0.08. $(k_V/k_H)_2$=0.05. $(k_V/k_H)_3$=0.03.

The thin curves of Figure 3.41 describe the response of the same horizontal well in the equivalent homogeneous layer. The two model responses appear very similar, the use of the *homogeneous layer* approximation is acceptable. For a n layer system, the average horizontal permeability is defined (Section 4.2.5) as:

$$\bar{k}_H = \sum_1^n k_i h_i \Big/ \sum_1^n h_i \tag{3.55}$$

For the vertical flow, the changes of permeability are acting in series. The resulting average vertical permeability estimated during the vertical radial flow is defined with the *average vertical* permeability above, and below the horizontal drain. If the well is centered in layer j :

$$\bar{k}_V = 0.5\left(\frac{\sum_1^{j-1} h_i + h_j/2}{\sum_1^{j-1} h_i/k_i + h_j/2k_j} + \frac{\sum_{j+1}^{n} h_i + h_j/2}{\sum_{j+1}^{n} h_i/k_i + h_j/2k_j}\right) \tag{3.56}$$

Equations 3.55 and 3.56 are applicable to the example Figure 3.41 with n=3 and j=2: $\bar{k}_H = 10.7$ and $\bar{k}_V = 0.5(0.82 + 0.28) = 0.55$.

On Figure 3.42, a low permeability zone is inserted in the producing interval: the horizontal well is located in layer 3, below the semi-permeable wall (layer 2). The response shows first the vertical radial flow regime around the wellbore in layer 3 and, when both the bottom boundary and the low permeability interbed are reached, it tends to deviates into a linear flow regime as if layer 3 was isolated (the thin dashed curves describe the response of the horizontal well if layer 2 is sealing). Later, a crossflow is established through the semi-permeable wall and layer 1 participates to the production.

The derivative deviates below the half-unit slope straight line in a transition, and finally reaches the stabilization when the flow becomes horizontal pseudo-radial.

A match of the stratified reservoir response with an equivalent homogeneous model is presented with the thin curves. The average horizontal permeability is defined by Equation 3.55. Due to the early deviation above the first derivative stabilization when the semi-permeable wall is reached, the effective well length used for this match is only 55% of the true length. L being *under estimated*, the vertical permeability resulting from the vertical radial flow stabilization is *too large* (3.8 times the vertical permeability in layers 1 and 3, and 6.7 times the average vertical permeability of Equation 3.56).

The presence of interbeds with very low k_V, in a otherwise homogeneous reservoir, affects the shape of horizontal well response curves and consequently the productivity. On the stratified reservoir example Figure 3.42, the total skin S_{TH} of the horizontal well is S_{TH} =-6.48. In case of a non-rectilinear well with a segment of L /2 in layers 1 and 3, the total skin would be lower at S_{TH} =-6.53 and, without layer 2 (homogeneous reservoir) it is S_{TH} =-6.78.

Kuchuk and Habashy (1996) use the layered reservoir model to describe the influence of a gas cap or bottom water drive on horizontal well responses. Since in the model boundaries between layers are horizontal planes, they assume that the interface between the fluids is not moving or distorted by cresting during the production. In the example of Figure 3.43, the horizontal well is located at the bottom of a layer overlaid by a gas cap. The sequence of regimes is vertical radial flow and hemi-radial flow until the gas interface is reached. Later, due to the large mobility and compressibility of the top gas region, the pressure tends to stabilize and shows the influence of a constant pressure boundary similar to the partial penetration example of Figure 3.21. If the thickness of the gas cap is not large enough, the response deviates from the constant pressure upper boundary behavior, and finally stabilizes to describe the total mobility of the oil and the gas zones.

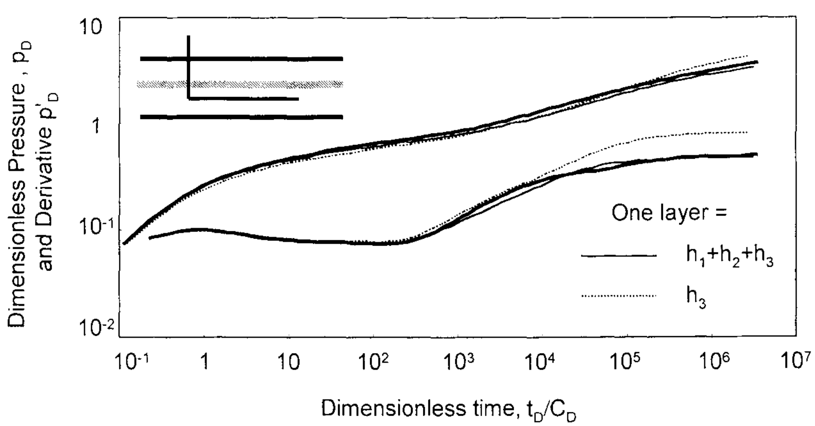

Figure 3.42. Horizontal well close to a low permeability interbed. Log-log scales. C_D =100, L =1000ft, S_w =0, h =100ft (45+5+50), r_w =0.25ft, z_w/h =0.25, $k_{H1}=k_{H3}$=100 k_{H2}, $(k_V/k_H)_i$=0.1.

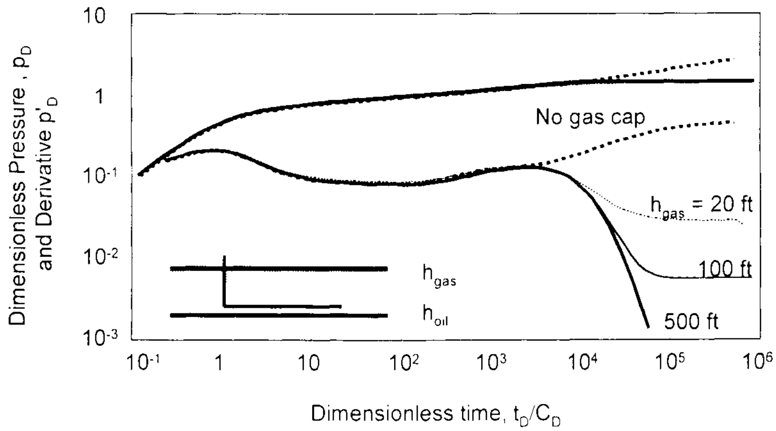

Figure 3.43. Horizontal well in a reservoir with gas cap. C_D =100, L =1000ft, S_w =2, h_{oil}=100ft, r_w =0.25ft, z_w/h_{oil}=0.2, $(k_V/k_H)_i$=0.1, h_{gas}/h_{oil} = 0.2, 1 and 5, μ_{gas}/μ_{oil} =0.01, c_{tgas}/c_{toil} =10.

Fleming et al. (1994) observed that many build-up tests from horizontal wells in a fissured reservoir with a large gas cap show several oscillations on the late time derivative response. They explain this phenomenon by the changes of saturation as the gas recedes during shut-in. The gas movement within the fracture network can be stepping, with intermittent liberation of gas pockets. Horizontal wells in double porosity reservoirs are further discussed in Section 4.1.4. In addition, multiphase reservoirs are presented in Chapter 8.

3.6.12 Multilateral horizontal wells

In single layer homogeneous reservoirs, the behavior of wells with multiple horizontal drain-holes follows a logic similar to partially open and multi-fractured horizontal wells, discussed in previous sections:

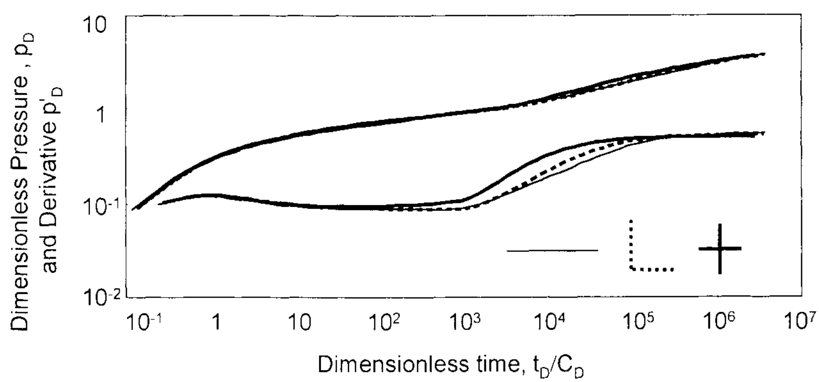

Figure 3.44. Multilateral horizontal well. Log-log scales, p_D versus t_D/C_D. C_D =100, L =1000ft (500+500 and 250+250+250+250), S_{wi} =0, h =100ft, r_w =0.25ft, k_V / k_H =0.1, z_w / h =0.5.

- At early time, the different branches produce *independently* and, when the different drain-holes have the same skin, the behavior is equivalent to a single horizontal well with a total effective length defined as the sum of the lengths of all branches.
- Later, the response deviates due to *interference effects* between the different horizontal sections. The flow geometry is a function of both horizontal and vertical distances between the branches, and orientation. An analytical simulator is required to properly interpret the well response.
- Finally, *pseudo radial flow* towards the multilateral horizontal well can develop.

On Figure 3.44, two examples of multilateral horizontal well responses are compared to the horizontal well of similar total length. The drain-hole sections are perpendicular with two and four branches (L and + shape). At intermediate time, the interference effects produce an increase of the pressure response, and the derivative deviates above the half unit slope straight line of the single drain horizontal well curve. No mechanical skin damage is assumed on the three curves. The total skin S_{TH} of the horizontal well is S_{TH} =-6.8 whereas for the multilateral well examples S_{TH} is respectively -6.6 and -6.2 with the L and + geometries.

For a given total effective length, increasing the number of intersecting branches does not improve the productivity of horizontal wells in reservoirs with isotropic horizontal permeability (Larsen, 1996 a; Salas et al., 1998). When the horizontal perforated segments do not intersect, Larsen shows that the total skin S_{TH} can be expressed as a function of the dimensionless distance r_D between the segments, with a decreasing function of ln r_D. On the examples Figure 3.45 where the distance between the two producing segments is large enough, the response becomes independent of the orientation of the branches and the total skin of the two multilateral horizontal wells is S_{TH}=-7.1 (more negative than S_{TH}=-6.8 with one branch). The responses Figure 3.45 tend to be equivalent to the example with two segments of Figure 3.37.

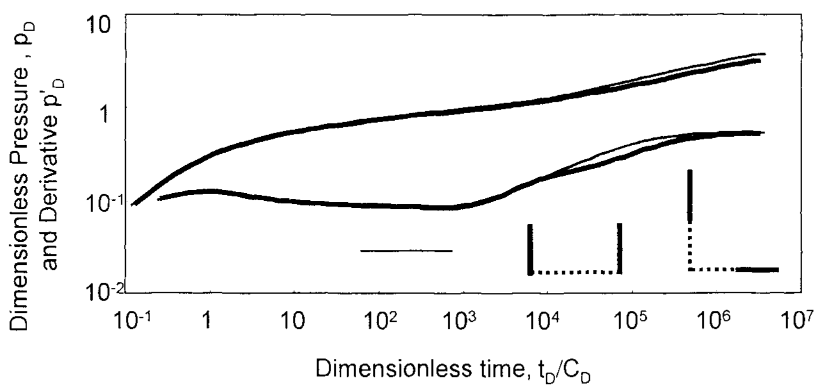

Figure 3.45. Multilateral horizontal well. Log-log scales. C_D=100, L =1000ft (500+500), S_{wi} =0, h =100ft, r_w =0.25ft, k_V/k_H =0.1, z_w/h =0.5. The distance between the 2 parallel branches is 2000ft, on the second example the intersection point is at 1000ft from the start of the 2 segments.

3.7 SKIN FACTORS

3.7.1 Components of the total skin

The different *components* contributing to the total skin S_T measured on well test responses are summarized on table 3.7 below.

Table 3.7. Components of the total skin S_T

Name	Description	Type
S_w	Infinitesimal skin at the wellbore.	Positive or negative
S_G	Geometrical skin due to the streamline curvature (fractured, partial penetration, slanted or horizontal wells).	Positive or negative
S_{ani}	Skin factor due to the anisotropy of the reservoir permeability.	Negative
S_{RC}	Skin factor due to a change of reservoir mobility near the wellbore (permeability or fluid property, radial composite behavior).	Positive or negative
$S_{2\phi}$	Skin factor due to the fissures in a double porosity reservoir.	Negative
$D.q$	Turbulent or inertial effects on gas wells.	Positive

The geometrical skin S_G has been discussed in previous Sections for various well configurations. In the following, the relationship between S_G and *derivative curves* is demonstrated by comparing three simple example responses. Negative skin produced by natural fissures is discussed in the double porosity Section 4.1.5, and turbulence effects are described in the gas well Chapter 7.

3.7.2 Geometrical skin and derivative curves

The magnitude of the geometrical skin is easy to visualize when the derivative response is considered. This can be illustrated by the theoretical response of three wells of radius r_w, producing in the same homogeneous reservoir (Figure 3.46). Well **A** is a fully penetrating *vertical well*, well **B** is in *partial penetration*, and well **C** is a *horizontal well*. For the three wells, the infinitesimal skin S_w is set to 0.

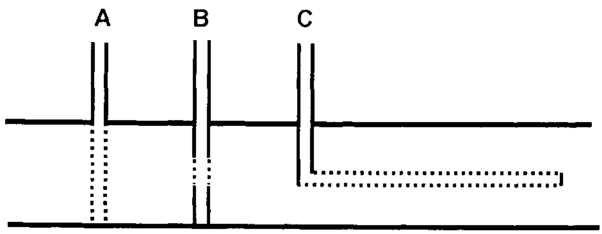

Figure 3.46. Configuration of well **A**, **B** and **C**.
A = fully penetrating vertical well, **B** = well in partial penetration and **C** = horizontal well.

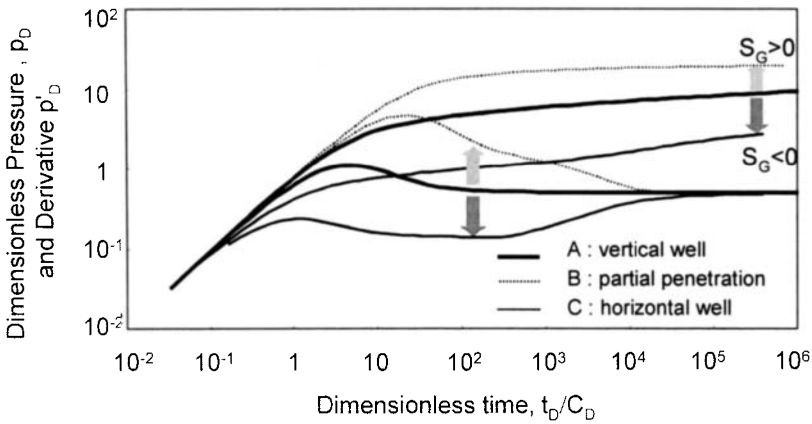

Figure 3.47. Pressure and derivative responses of well **A** (vertical), **B** (partial penetration) and **C** (horizontal). Log-log scales, p_D versus t_D/C_D.

In Figure3.47, the derivative response of the vertical well shows the usual stabilization when the wellbore storage is over. In the case of partial penetration well **B**, a first derivative stabilization is seen during the radial flow in front of the perforated interval. The derivative response is above that of the vertical well until $t_D/C_D = 10^4$, the *area* between the two curves is a measure of the positive geometrical skin. The larger this surface, the larger is the skin due to partial penetration. In terms of pressure response, the partial penetration curve **B** is above the curve for the vertical well.

For the horizontal well **C**, the derivative response stabilizes at a low level during the vertical radial flow and the resulting geometrical skin is negative. The longer is the horizontal well, the larger is the area below the vertical well derivative response, and the more negative is the total skin.

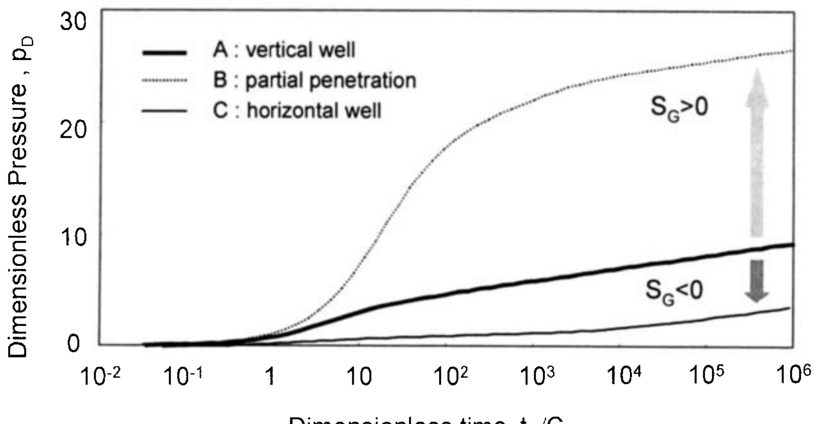

Figure 3.48. Semi-log plot of Figure 3.47 examples.

The influence of the geometrical skin on the pressure response of wells **A**, **B** and **C** is illustrated on semi-log scale Figure 3.48.

This Page Intentionally Left Blank